MAGNETIC RESONANCE IN CHEMISTRY
Magn. Reson. Chem. **36**, S93–S103 (1998)

Ab initio IGLO studies of the conformational dependences of ^{13}C NMR chemical shifts and α-through ε-substituent effects in 1-substituted pentanes†

Michael Barfield*

Department of Chemistry, University of Arizona, Tucson, Arizona 85721, USA

Received 8 December 1997; accepted 26 January 1998

ABSTRACT: *Ab initio* IGLO (individual gauge for localized molecular orbital) methods of SCF-MO theory were used to extend studies of the conformational dependences of isotropic ^{13}C NMR chemical shifts to *n*-hexane and three 1-substituted pentanes $XCH_2CH_2CH_2CH_2CH_3$ (X = CN, OH, F). Isotropic shifts were obtained as a function of the torsion angles φ_1, φ_2 and φ_3 measured about the C1—C2, C2—C3 and C3—C4 bonds, respectively, with molecular structures optimized at the HF/6–31G* level. The calculated ^{13}C chemical shifts and substituent effects, averaged over the torsional motions, compare favorably with the experimental data. The computed stereochemical dependencies of α- through ε-effects are compared with experimental values in several series of bicyclic molecules which encompass a range of the three torsion angles. Emphasized here are δ- and ε-effects, which are sensitive to all three dihedral angles. Inclusion of the third dihedral angle improves the results over those based on the substituted *n*-butanes, especially for δ-methylene carbons which can be shielded or deshielded depending on φ_3. Analysis of the IGLO local bond contributions in sterically crowded conformations suggests a general tendency in which C—H bonds pointing toward and away from the substituent lead to deshielding and shielding, respectively.

KEYWORDS: conformational dependences; ^{13}C NMR chemical shifts; 1-substituted pentanes; α-, β-, γ-, δ- and ε-substituent effects; *ab initio* IGLO computations; conformational averaging

INTRODUCTION

Substituent effect $\Delta\delta_i$ ($i = \alpha, \beta, \gamma, \delta, \varepsilon$, etc.) in the ^{13}C NMR spectra of aliphatic and alicyclic compounds are the changes in the chemical shifts δ_i of carbon C*i* which occur on replacing a hydrogen atom at the C_α carbon by a substituent X.[1] For some substituents $\Delta\delta_\alpha$ can be very large but the magnitude of the effects decreases along the chain such that the $\Delta\delta_\varepsilon$ are usually considered to be negligible. Even at an early stage in these studies, γ-substituent effects were of particular interest not only because they were in a direction generally opposite to the other effects but also exhibited a strong stereochemical dependence.[1,2] The characterization and discussions of the source of the various substituent effects have been of great interest. It is appropriate here to mention several relevant studies from the laboratory of J. D. Roberts.[3] Empirical additivity relationships based on the tabulated substituent effects are very useful in the interpretation of ^{13}C NMR spectra.[4–8] The dependences of γ- and δ-substituent effects on stereochemical features were recognized at an early stage, and the conformational implications of the various substituent effects are of particular interest.[9–11]

A series of papers from these[12–17] and other[18] laboratories have made use of *ab initio* MO methods to investigate the structural and conformational dependences of ^{13}C NMR chemical shifts and substituent effects. The IGLO method was used to examine the torsion angle (φ about C2—C3) dependence of α-, β- and γ-effects for *n*-butane.[12] Satisfactory agreement was found with the experimental data for *n*-butane but not for the methyl-substituted bicyclic compounds with reasonably well defined geometry. Extension of the analysis of γ-effects to include branching along the chain (in, e.g., 2,3-dimethylbutane) led to satisfactory agreement with the experimental data (for several series of methyl-substituted bicyclic compounds) and to different conformational dependences for *threo* and *erythro* arrangements.[13] A subsequent IGLO study of *n*-pentane and three substituted butanes (X = CN, OH, F) examined the dependence of α-, β-, γ- and δ-effects on the torsion angles φ_1 and φ_2 about the C1—C2 and C2—C3 bonds, respectively.[16] In contrast to β-effects which were found to be almost independent of φ_2, the calculated α-, γ- and δ-effects showed substantial variations with both dihedral angles. The predicted dependences of substituent and conformational effects were consistent with the experimental results for several series of substituted bicyclo[2.2.1]heptanes, bicyclo[2.2.2]octanes and *trans*-decalins. Of particular interest in this regard were the conformational dependences of γ- and δ-effects on φ_1 and φ_2 in which both the calculated IGLO results and the experimental data

* *Correspondence to*: M. Barfield, Department of Chemistry, University of Arizona, Tucson, Arizona 85721, USA
† Dedicated to Professor John D. Roberts on the Occasion of his 80th birthday
Contract/grant sponsor: National Science Foundation.

CCC 0749-1581/98/SI0093–11 $17.50

exhibit substantially more positive values in sterically crowed g^+g^- arrangements than for g^+g^+ and g^+t arrangements. For δ-methyl carbons the calculated results were consistent with the experimental data including the 2–3 ppm deshielding effects in *syn*-axial (g^+g^-) arrangements.

The computational methods used for molecular structures and chemical shielding are presented in the next section. Then the calculated ^{13}C isotropic ^{13}C NMR chemical shifts and α- through ε-substituent effects for the 1-substituted pentanes are compared with the experimental data. In the subsequent section the calculated conformational and substituent dependences are compared with the representative experimental data for a series of 'rigid' bicyclic molecules as a function of the three dihedral angles. Since the conformational dependences of δ- and ε-effects are of particular interest, results for *n*-hexane as a representative example are depicted by surface and contour plots. An analysis of the IGLO local bond contributions suggests that in sterically crowded situations the shortened C—H bonds pointing toward and away from the substituent lead to deshielding and shielding effects, respectively.

COMPUTATIONS

Molecular Structures

All geometries are optimized ones using Gaussian 92[19] and Gaussian 94[20] codes with split valence basis sets and polarization functions at the HF/6–31G* level.[21] Calculations for *n*-hexane (**2**), hexanenitrile (**3**), pentan-1-bl (**4**) and 1-fluoropentane (**5**) were performed at 60° intervals of the three dihedral angles φ_1, φ_2, and φ_3. All geometries are fully optimized (except for the three dihedral angles) at the HF/6–31G* level. The *n*-pentane data were taken from a previous study.[16] For each of the 1-substituted pentanes, the 60° grid implies 216 structures but only 112 were actually calculated as the rest are symmetry related. The additional symmetry of *n*-hexane further reduces the number of data points required. The use of such a coarse grid is not usually desirable, but a 30° grid would have increased the computational effort by a factor of eight. Also, most of the experimental data occur for molecules having dihedral angles fairly close to those in the 60° grid.

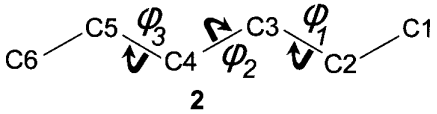

2

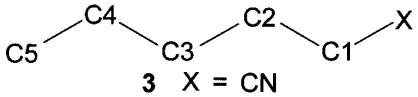

3 X = CN
4 X = OH
5 X = F

Shielding Calculations

All shielding calculations in this study were based on the IGLO (individual gauge for localized orbitals) formulation of Kutzelnigg *et al.*[22,23] This procedure has been applied with success to a large number of molecules having elements in the first through third rows. In this method, localized MOs, which are associated with inner shells, bonding orbitals and lone pairs, have unique gauge origins for the calculation of diamagnetic and paramagnetic terms. Distributed origins algorithms such as IGLO, LORG[24] and GIAO[25] provide a satisfactory description of chemical shielding using modest basis sets.[22–26] In the notation of the Bochum group,[22,23] Basis Set II is a (9/5) set contracted to a triple-ζ (51111/2111) set with one set of (5) *d*-type functions on elements C–F and for hydrogen a (311) set with *p*-type polarization functions.[27] All IGLO calculations here were performed with Basis Set II′, which differs from Basis Set II in using a double-ζ set on hydrogen. The ^{13}C shielding results with the two basis sets are comparable. The basis set dependences of chemical shifts have been extensively discussed,[22–26] including a related one from this laboratory[14] which compared IGLO Basis Set I, II′ and II results with the experimental data for substituted cyclobutanes.

All chemical shifts were obtained by subtracting the chemical shielding for the nuclei of interest from the reference compound shielding (tetramethylsilane, TMS). A 194.0 ppm value for the ^{13}C TMS shielding was inferred from the computed methane shielding (201.0 ppm for Basis Set II′ and HF/6-31G* geometry) and the experimental chemical shift (−7.0 ppm)[28] for gas-phase CH_4 relative to TMS in solution. Previous IGLO results for isotropic ^{13}C chemical shifts from this laboratory[13–17] used an early criterion from the Bochum group[22] in which −2.3 ppm was adopted for the methane reference. With this value, for example, the average deviation between calculated (IGLO, with a triple-ζ basis set) and experimental ^{13}C shifts for 16 carbons in a series of 1-substitued butanes was +2.2 ppm.[16] Based on the −7.0 ppm value for gas-phase methane, the average deviation for the same set of data is −2.5 ppm. All computations were performed using Convex C220 and C240 minisupercomputers or IBM/590 RISC6000 workstations. The 3D surface and contour plots were generated by a commercial plotting package which includes 2D and 3D spline algorithms (cubic or bicubic spline interpolation).[29] For *n*-hexane and the 1-substituted pentanes the conformationally averaged shifts $\langle\delta_i\rangle$ were calculated as the average of the chemical shift surfaces $\delta_i(\varphi_1, \varphi_2, \varphi_3)$ over the corresponding energy surface $E_i(\varphi_1, \varphi_2, \varphi_3)$,

$$\langle\delta_i\rangle = \frac{\int \delta_i(\varphi_1, \varphi_2, \varphi_3) e^{-E_i(\varphi_1, \varphi_2, \varphi_3)/kT} d\varphi_1 d\varphi_2 d\varphi_3}{\int e^{-E_i(\varphi_1, \varphi_2, \varphi_3)/kT} d\varphi_1 d\varphi_2 d\varphi_3} \quad (1)$$

The averaged chemical shifts in the next section were obtained by numerical integration using Eqn (1).

Previously, it was noted that the use of fully optimized structures subject only to the dihedral angle constraints presents problems in the interpretation of the chemical shifts because the remaining $3N - 8$ internal degrees vary in each structure. Clearly, this leads to uncertainties in separating the importance of the fixed dihedral angles from the concomitant changes in bond lengths, internal angles and other dihedral angles. On the other hand, constraining certain bond lengths and internal angles leads to unphysical values of energies and chemical shifts, especially in the interesting strained conformations.[16]

COMPARISONS OF CALCULATED CHEMICAL SHIFTS WITH EXPERIMENTAL DATA FOR THE 1-SUBSTITUTED PENTANES

The calculated IGLO isotropic ^{13}C NMR chemical shifts and the experimental data for all carbons in **1**–**5** are presented in Table 1. The notation IGLO/BS II′// HF/6–31G* is used to denote IGLO Basis Set II′ calculations performed for structures optimized at the HF/6–31G* level. The calculated chemical shifts $\delta_i^{\min}$ in the lowest energy conformations (HF/6–31G*) are entered in the third column. Except for the C1 carbons of pentan-1-ol and 1-fluoropentane, the agreement with the experimental data in column 5 is satisfactory considering that the calculated values apply to the gas-

Table 1. Comparison of calculated chemical shift (IGLO Basis Set II′) averages for pentane and substituted pentanes (HF/6–31G* optimized geometries) with solution NMR data[a]

			$\langle\delta_i\rangle$		$\langle\Delta\delta_i\rangle$		
Compound[b]	Carbon	$\delta_i^{\min}$	Calc.	Expt.	Calc.[c]	Expt.[c]	Empirical[d]
n-Pentane[e]	C1	12.5	11.9	14.2 (13.87)[f]			
	C2	21.1	19.7	23.1 (22.33)			
	C3	30.5	29.3	35.0 (34.18)			
	C4	21.1	19.7	23.1 (22.33)			
	C5	12.5	11.9	14.2 (13.87)			
n-Hexane[g]	C1	12.6	12.0	14.4 (13.7)[h]			
	C2	21.1	20.1	23.5 (22.8)	8.2	9.3 (9.2)[h]	9.1
	C3	29.4	27.7	32.5 (31.9)	8.0	8.8 (9.5)	9.4
	C4	29.4	27.7	32.5 (31.9)	−1.6	−2.5 (−2.5)	−2.5
	C5	21.1	20.1	23.5 (22.8)	0.4	0.4 (0.4)	0.3
	C6	12.6	12.0	14.4 (13.7)	0.1	0.2 (0.2)	—
Hexanenitrile[i,j]	C1	14.3	13.9	17.1	2.0	3.2	3.1
	C2	24.8	23.1	25.4	3.4	3.1	2.4
	C3	28.4	26.3	31.0	−3.0	−3.2	−3.3
	C4	20.5	19.4	22.0	−0.3	−0.3	−0.5
	C5	12.3	11.8	13.8	−0.1	−0.1	—
	CN	121.2	121.3	119.7	—	—	—
1-Pentanol[k]	C1	55.5	55.5	62.5 (61.8)[l]	43.6	48.3 (48.4)[l]	49.1
	C2	27.9	27.0	33.2 (32.5)	7.3	10.1 (10.2)	10.1
	C3	24.9	23.9	29.0 (28.2)	−5.4	−6.0 (−6.0)	−6.2
	C4	20.8	19.8	23.4 (22.6)	0.1	0.3 (0.3)	0.3
	C5	12.6	12.0	14.4 (13.8)	−0.5	0.2 (0.4)	—
1-Fluoropentane[m]	C1	74.9	74.6	84.3	62.7	70.4	70.1
	C2	27.9	26.8	31.1	7.1	8.8	7.8
	C3	24.7	23.6	28.3	−6.9	−5.9	−6.8
	C4	20.7	19.6	23.2	−0.1	0.9	0.0
	C5	12.5	11.9	14.2	0.0	0.3	—

[a] All values in ppm referenced to TMS.
[b] Unless specified otherwise, the data were taken from T. Pehk and E. Lippmaa, *Org. Magn. Reson.* **3**, 679 (1971).
[c] These values were obtained by subtracting the pentane chemical shifts from those of the substituted pentanes.
[d] Ref. 6.
[e] Minimum energy (HF/6–31G*): −196.333 096 5 hartree at $\varphi_1 = \varphi_2 = 180°$.
[f] K. B. Wiberg, W. E. Pratt and W. F. Bailey, *J. Org. Chem.* **45**, 4936 (1980).
[g] Minimum energy (HF/6–31G*): −235.367 791 6 hartree at $\varphi_1 = \varphi_2 = \varphi_3 = 180°$.
[h] D. M. Grant and E. G. Paul, *J. Am. Chem. Soc.* **86**, 2984 (1964). Chemical shifts converted to the δ-scale with benzene at δ 128.5.
[i] Minimum energy (HF/6–31G*): −288.067 464 9 hartree at $\varphi_1 = \varphi_2 = \varphi_3 = 180°$.
[j] Sadtler Research Laboratories, *Atlas of ^{13}C NMR Data*, No. 456C.
[k] Minimum energy (HF/6–31G*): −271.179 993 0 hartree at $\varphi_1 = 60°$, $\varphi_2 = \varphi_3 = 180°$.
[l] J. D. Roberts, F. J. Weigert, J. I. Kroschwitz and H. J. Reich, *J. Am. Chem. Soc.* **92**, 1338 (1970). Chemical shifts converted to the δ-scale with CS_2 at δ 192.5.
[m] Minimum energy (HF/6–31G*): −295.182 154 2 hartree at $\varphi_1 = 60°$, $\varphi_2 = \varphi_3 = 180°$.

phase molecules and all NMR data were measured in solution. The standard deviation between the calculated and experimental values is 2.2 ppm. This drops to 1.4 ppm for all 20 distinct carbons not including the C1 carbons of **4** and **5**. The optimized geometries around heteroatoms are sensitive to basis set quality. It seems likely that the disparities at the C1 carbon of **4** and **5** would be improved by performing the geometry optimizations and shielding calculations with larger basis sets.[17]

To investigate the importance of the torsional motions about the three C—C single bonds to the isotropic ^{13}C NMR shifts, average values $\langle\delta_i\rangle$ were obtained by three-dimensional numerical integration using Eqn (1) (at 300 K), the calculated shift data δ_i (φ_1, φ_2, φ_3) for each of the carbons and the HF/6-31G* potential energy data $E_i(\varphi_1, \varphi_2, \varphi_3)$. The averaged chemical shifts $\langle\delta_i\rangle$ are entered in the fourth column of Table 1. Relative to the chemical shifts computed at the minimum energy geometries, averaging has the effect of decreasing the calculated results by as much as 2.1 ppm, but an average by 0.9 ppm. Since the δ_i^{min} values (with one exception) are less than the experimental solution values, torsional averaging does not improve the overall agreement between the calculated and experimental results. Almost certainly this is an artifact of both the way in which the shifts are referenced and inadequacies at this level of theory. The standard deviation between the calculated $\langle\delta_i\rangle$ and experimental values in Table 1 is 2.3 ppm ($r^2 = 0.992$). If the C1 carbons of **4** and **5** are not included, this drops to 1.6 ppm $r_2 = 0.996$), which is somewhat less than recent results using DFT/GIAO methods to calculate ^{13}C isotropic chemical shifts in substituted benzenes and pyrimidines.[17] As noted previously,[16] torsional averaging is more important for the interior (C2, C3 and C4 carbons of *n*-hexane, for example) carbons than for the terminal (C1 and C6) carbons. Also included in Table 1 for each of the four substituents are the calculated and experimentally inferred values $\langle\Delta\delta_i\rangle$ for the α- through ε-effects. The calculated values were obtained from the torsion averaged ^{13}C NMR chemical shifts $\langle\delta_i\rangle$, but the results based on δ_i^{min} are comparable. Except for carbons in proximity to the fluoro-substituents, the agreement is good (in fact, the standard deviation for all 20 entries is 0.6 ppm ($r^2 = 0.998$). The empirical values for α-through δ-effects are comparable.

CONFORMATIONAL AND SUBSTITUENT DEPENDENCES OF α- THROUGH ε-EFFECTS. COMPARISONS WITH SUBSTITUENT DEPENDENCES IN CYCLIC MOLECULES

This section includes a discussion of the conformational dependences for **2**–**5** and a comparison of calculated results with experimental data for monosubstituted cyclic and bicyclic molecules. Of interest for ε- effects are comparisons with data for several 'rigid' dimethyl- and hydroxy-substituted bicyclic compounds having ε-carbons as methyl groups. The calculated α- through ε-effects $\Delta\delta_i$ (φ_1, φ_2, φ_3) of the four substituent groups in **2**–**5** were obtained by subtracting the IGLO shielding results σ_i (φ_1, φ_2, φ_3) for the C1–C5 (C2–C6 for **2** and **3**) carbons from the corresponding *n*-pentane values. These data $\Delta\delta_i$ are entered in Table 2 for the 14 'standard' structures depicted in Fig. 1. Also included, to show the importance to the calculated substituent shifts of introducing a third dihedral angle, are the α- through δ-effects for the substituted butanes in the five 'standard' conformations (g^+g^+, g^+t, g^+g^-, tg^+ and tt). These were obtained at the same level of theory.[16]

The IGLO α- through ε-substituent effects in Table 1 are in reasonable agreement with the experimental data. With increasing substituent electronegativity (neglecting the nitrile data), the averaged α-effects increase substantially, β-effects decrease slightly, γ-effects become more negative and the δ-effects are probably too small to exhibit a clear trend. The data in Table 2 show that substituent trends can be conformation dependent. To see how well the calculated dependences compare with those observed, it is necessary to find chemical shift

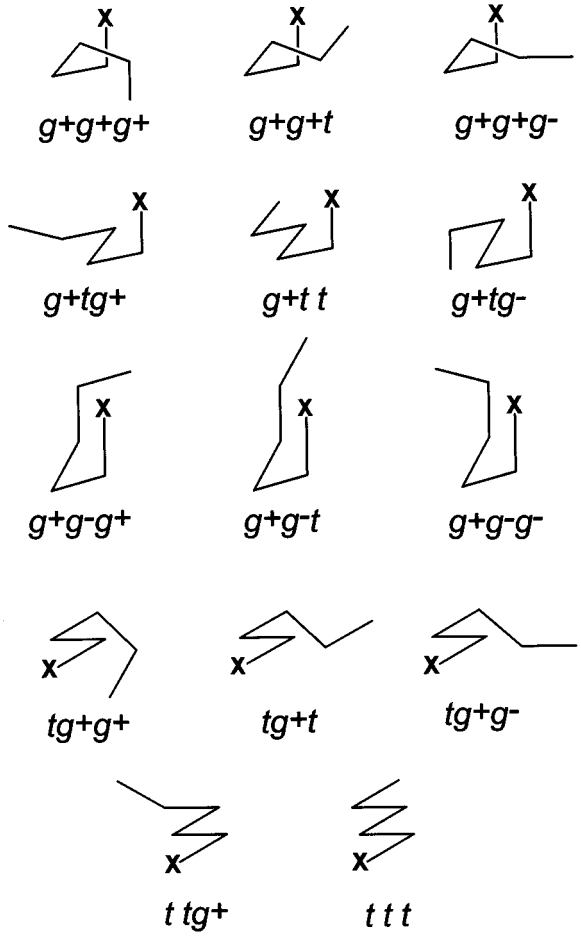

Figure 1. Schematic representations of the 14 standard arrangements for the C—C—C—C—C—X moiety of 1-substituted pentanes in cyclic molecules.

Table 2. Calculated values (IGLO/BS II′//HF/6–31G*) of α- through ε-substituent effects in *n*-hexane and 1-substituted pentanes for the conformations depicted in Fig. 1[a]

	Hexane					Hexanenitrile					Pentan-1-ol					1-Fluoropentane				
	$\Delta\delta_\alpha$	$\Delta\delta_\beta$	$\Delta\delta_\gamma$	$\Delta\delta_\delta$	$\Delta\delta_\varepsilon$	$\Delta\delta_\alpha$	$\Delta\delta_\beta$	$\Delta\delta_\gamma$	$\Delta\delta_\delta$	$\Delta\delta_\varepsilon$	$\Delta\delta_\alpha$	$\Delta\delta_\beta$	$\Delta\delta_\gamma$	$\Delta\delta_\delta$	$\Delta\delta_\varepsilon$	$\Delta\delta_\alpha$	$\Delta\delta_\beta$	$\Delta\delta_\gamma$	$\Delta\delta_\delta$	$\Delta\delta_\varepsilon$
g^+g^+	5.9	5.7	−4.3	−0.5	—	1.8	3.1	−3.7	−0.5	—	42.3	6.7	−5.6	−0.6	—	62.0	6.6	−5.6	−0.7	—
$g^+g^+g^+$	5.6	5.7	−4.8	−0.4	0.4	1.6	3.1	−4.2	−0.6	0.1	42.1	6.6	−6.0	−0.4	0.5	61.9	6.7	−6.0	−0.6	0.4
g^+g^+t	5.4	5.8	−4.9	−0.5	0.0	1.3	3.2	−4.6	−0.4	−0.4	41.7	6.8	−6.2	−0.6	−0.1	61.4	6.7	−6.3	−0.8	−0.2
$g^+g^+g^-$	5.9	6.1	−5.0	0.2	−1.1	1.4	3.1	−4.5	−0.9	−1.3	41.7	6.8	−6.2	−0.8	−1.3	61.3	6.9	−6.0	−1.2	−0.8
g^+t	6.6	6.1	−4.5	0.1	—	1.9	2.4	−3.8	−0.7	—	43.0	6.7	−5.5	−0.3	—	62.4	6.7	−5.6	−0.5	—
g^+tg^+	6.4	5.9	−4.7	−0.1	0.0	1.7	2.8	−4.2	−0.7	−0.4	42.8	6.8	−5.9	−0.3	−0.1	62.2	6.8	−5.9	−0.5	−0.2
g^+tt	6.6	6.0	−4.5	0.2	0.1	1.8	2.6	−4.2	−0.6	−0.3	42.9	6.8	−5.7	−0.3	0.1	62.3	6.8	−5.8	−0.5	−0.1
g^+tg^-	6.5	5.8	−4.6	0.0	−0.1	1.9	3.0	−3.8	−0.7	−0.1	43.2	6.8	−5.6	−0.5	0.0	62.6	7.1	−5.6	−0.7	−0.1
g^+g^-	10.4	6.5	0.3	2.6	—	3.2	2.6	−0.2	0.7	—	47.4	6.6	0.1	2.4	—	66.4	6.6	−0.7	2.0	—
$g^+g^-g^+$	5.6	6.7	0.0	−1.9	0.9	0.3	3.4	−0.9	−1.6	0.0	42.1	7.0	−0.6	−0.8	−0.4	60.8	6.7	−1.4	−1.4	−1.3
g^+g^-t	9.3	6.4	0.4	1.6	0.7	2.3	2.6	−0.6	−0.4	0.2	46.2	6.8	−0.3	1.3	0.6	65.3	6.8	−1.2	1.2	0.4
$g^+g^-g^-$	10.8	6.3	0.3	3.0	0.9	3.3	2.7	−0.6	0.3	0.6	47.6	7.1	−0.2	2.6	0.6	66.8	7.0	−0.9	2.2	0.5
tg^+	8.4	8.3	−0.3	0.6	—	2.5	4.1	−1.2	−0.2	—	45.6	7.5	−3.4	0.9	—	65.1	6.0	−4.2	0.7	—
tg^+g^+	8.0	8.3	−0.7	0.5	0.1	2.1	4.3	−1.6	−0.1	−0.2	45.1	7.6	−3.8	1.1	0.1	64.5	7.0	−5.0	0.8	0.0
tg^+t	7.9	8.4	−0.8	0.5	0.1	1.9	4.2	−1.9	−0.2	−0.3	44.8	7.5	−3.8	0.9	0.2	64.0	6.8	−5.1	0.6	0.1
tg^+g^-	7.2	9.0	−0.9	−0.2	0.2	1.3	4.4	−2.0	−1.0	0.0	43.3	8.0	−3.6	−0.7	−0.1	62.4	7.5	−4.6	−1.0	−0.1
tt	8.6	8.3	−1.1	0.0	—	1.8	3.6	−1.9	−0.6	—	44.3	7.3	−5.9	−0.3	—	62.7	6.8	−7.5	−0.5	—
ttg^+	8.7	8.3	−1.2	0.0	0.0	1.8	4.2	−2.0	−0.5	−0.2	44.5	7.6	−6.1	−0.3	0.0	63.0	7.1	−7.8	−0.6	−0.1
ttt	8.6	8.3	−1.2	0.0	0.0	1.8	3.7	−2.2	−0.6	−0.2	44.3	7.4	−6.0	−0.3	0.1	62.7	7.2	−7.4	−0.6	−0.4
ttg^-	8.7	8.3	−1.1	0.0	0.0	1.8	4.2	−1.9	−0.5	−0.2	44.5	7.6	−6.0	−0.3	0.0	63.0	7.1	−7.7	−0.6	−0.1

[a] All values in ppm. Also included are values computed for *n*-pentane and the 1-substituted butanes.[16]

data for suitably rigid compounds with each of the four substituents. Unfortunately, actual molecules have one or more tertiary or quaternary carbons. The implications of branching on α- through δ-effects was noted previously[13,16] and will not be repeated here. Table 3 presents a comparison of the IGLO substituent effects with the available experimental data for several substituted bicyclic molecules having substituents CH_3, CN, OH and F. Nitrile and fluorine groups were included here because they often provide extremes for the influence of substituent effects but fewer experimental data are available. Substituent shifts in Table 3 include those for the 1-substituted bicyclo[2.2.2]octanes (BO), 1- and 2-substituted *trans*-decalins (TD) and 2-substituted bicyclo[2.2.1]heptanes (BH). These data were used previously for comparison with the IGLO α- through δ-effects of the 1-substituted butanes.[16] Additional entries in Table 3 are those for axial and equatorial cyclohexanes (CH) and several 3-substituted *trans*-decalins (TD). The dihedral angles in columns 2–4 were obtained for the fully optimized structures at the HF/6–31G* level. From Table 3, it can be seen that substituent-induced changes of φ_1 are as large as 10° whereas changes in φ_2 and φ_3 are less than 3°.

The calculated α- through ε-substituent effects in Table 3 were obtained from tables which were generated using 5° spline interpolation for the dihedral angles φ_1 and φ_2 with φ_3 fixed at angles in the 60° grid. This is a reasonable approximation since only one of the φ_3 values in Table 3 differs from the grid values by more than 6°. Most of the entries in Table 3 involve six-membered rings with no ε-carbons. The ε-effects are

Table 3. Comparison of calculated substituent effects (IGLO/BS II′//HF/6–31G*) for a series of 1-substituted pentanes with experimental data for a series of substituted bicyclic compounds[a]

	Dihedral angles[c]			$\Delta\delta_\alpha$		$\Delta\delta_\beta$		$\Delta\delta_\gamma$		$\Delta\delta_\delta$		$\Delta\delta_\varepsilon$	
Compound[b]	φ_1	φ_2	φ_3	Calc.	Expt.	Calc.	Expt.	Calc.	Expt.	Calc.	Expt.	Calc.	Expt.
2*n*-Me-BH	58	70	1	5.5	4.4	6.0	5.4	−5.2	−7.5	0.0	0.6	—	—
2*n*-CN-BH	56	71	0	1.4	0.1	3.1	3.4	−4.5	−4.9	−0.8	−0.7	—	—
2*n*-OH-BH	53	71	−1	41.5	43.3	6.6	6.2	−6.9	−9.6	0.0	0.3	—	—
1-Me-TD	68	54	308	6.2	−9.8	6.6	7.8	−4.3	−4.8	0.2	0.3	—	—
1-OH-TD	61	55	306	41.8	26.5	6.9	0.6	−5.9	−5.6	−0.8	−0.5	—	—
1-F-TD	63	54	305	61.2	49.5	6.8	3.3	−5.9	−4.8	−1.2	−0.5	—	—
1ax-Me-CH[d]	74	55	305	6.4	1.1	6.9	5.2	−4.2	−5.9	0.2	0.2	—	—
1ax-CN-CH[e]	70	54	305	1.7	0.1	3.6	−0.9	−4.1	−4.5	−0.8	−1.4	—	—
1ax-OH-CH[f]	68	55	305	42.3	37.8	7.5	5.5	−5.5	−6.8	−0.7	−0.7	—	—
1ax-F-CH[e]	66	54	305	61.9	61.1	7.6	3.1	−5.5	−7.2	−1.2	−2.0	—	—
2ax-Me-TD	55	176	66	6.2	−1.3	5.6	2.8	−5.0	−2.8	−0.1	0.4	0.0	0.0
2ax-OH-TD	55	179	65	42.5	36.1	6.4	3.7	−6.2	−4.7	−0.3	−0.1	−0.2	−0.5
3ax-Me-TD	74	179	180	7.2	1.5	6.9	5.6	−3.6	−6.7	0.2	0.1	0.1	0.0
3ax-OH-TD	72	179	180	44.0	39.7	7.9	6.1	−4.5	−7.3	−0.3	−1.4	0.1	−0.2
2eq-Me-TD	58	179	305	6.5	3.4	5.8	6.0	−4.6	−3.8	0.0	0.1	−0.1	−0.1
2eq-OH-TD	56	180	305	43.2	40.3	6.8	6.7	−5.7	−5.2	−0.5	−0.5	0.0	−0.7
1-Me-BO	180	0	60	7.4	3.4	9.3	7.3	0.4	0.7	0.2	0.7	—	—
1-CN-BO[g]	180	0	60	2.1	2.6	4.8	3.2	−0.6	−1.7	−0.7	−1.8	—	—
1-OH-BO	180	0	60	43.9	44.5	8.3	6.5	−1.6	−0.2	−0.1	−0.1	—	—
1-F-BO	180	0	60	63.3	69.8	7.8	4.9	−2.2	1.1	−0.4	0.0	—	—
2*x*-Me-BH	164	71	2	8.0	6.8	8.9	6.7	−0.8	0.4	−0.2	0.9	—	—
2*x*-CN-BH	167	72	0	1.4	1.0	4.8	5.5	−1.9	−1.5	−0.5	−1.6	—	—
2*x*-OH-BH	166	72	−1	44.0	45.1	8.3	7.9	−4.1	−5.2	−0.2	−1.5	—	—
2*x*-F-BH	174	73	−3	62.3	65.9	7.3	5.3	−5.8	−7.7	−0.4	−2.0	—	—
1eq-Me-CH[d]	181	55	305	7.0	6.4	9.0	8.5	−0.8	−0.4	−0.2	−0.1	—	—
1eq-CN-CH[e]	180	55	305	1.4	1.4	4.4	2.8	−2.0	−1.9	−1.0	−1.9	—	—
1eq-OH-CH[e]	185	55	305	43.3	42.6	8.1	8.0	−3.5	−2.7	−0.7	−2.0	—	—
1eq-F-CH[e]	177	55	305	62.6	64.5	7.6	5.6	−4.2	−3.4	−1.0	−2.5	—	—
3eq-Me-TD	179	180	180	8.6	6.0	8.3	8.7	−1.2	−0.6	0.0	−0.2	0.0	−0.2
3eq-OH-TD	180	180	180	44.3	43.3	7.4	8.7	−6.0	−2.5	−0.3	−1.0	0.1	−0.6

[a] Angles are in degrees and substituent effects in ppm.
[b] Unless noted otherwise, data were obtained from J. R. Whitesell and M. A. Minton, *Stereochemical Analysis of Alicyclic Compounds by C-13 NMR Spectroscopy*. Chapman and Hall, New York (1987).
[c] Dihedral angles are from geometries fully optimized at the HF/6–31G* level. These were used in conjunction with tables using 5° spline interpolation for φ_1 and φ_2. The φ_3 values are those in the 60° grid.
[d] H. Booth, J. R. Everett and R. A. Fleming, *Org. Magn. Reson.* **12**, 63 (1979).
[e] H.-J. Schneider and V. Hoppen, *Tetrahedron Lett.* 579 (1974).
[f] J. B. Stothers, Ref. 4, p. 65.
[g] E. W. Della and H. Gangodawila, *Aust. J. Chem.* **42**, 1485 (1989).

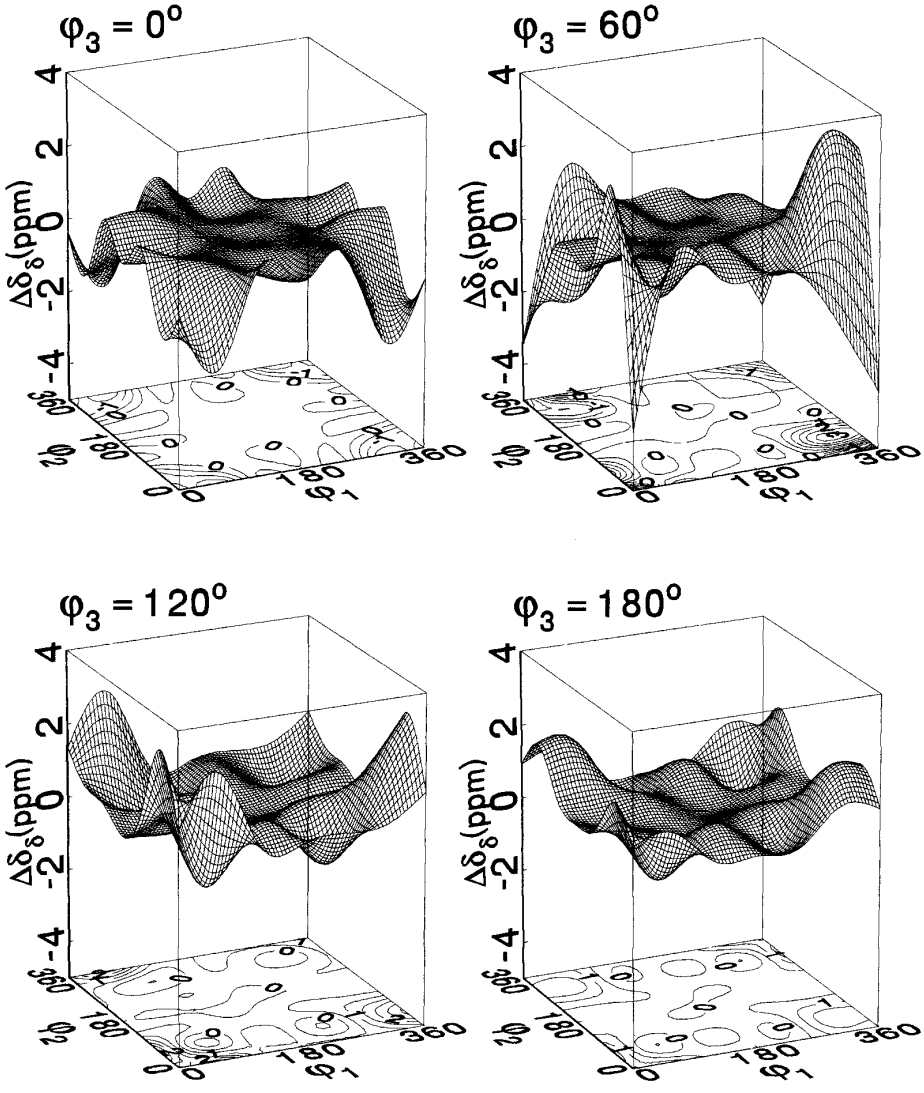

Figure 2. Calculated (IGLO/BS II′//HF/6–31G*) surface and contour plots of δ-effects $\Delta\delta_\delta$ in ppm for the C5 carbon of *n*-hexane (**2**) plotted as a function of the dihedral angles φ_1 and φ_2 measured about the C2—C3 and C3—C4 bonds, respectively, for 0°, 60°, 120° and 180° values of φ_3 measured about the C4—C5 bond. The contour lines are separated by 0.5 ppm.

given for several of the *trans*-decalins which have the substituent and the ε-carbon (methylene) in different rings. These are probably inappropriate comparisons since the calculated values apply to ε-methyl carbons.

α-, β- and γ-Effects

Since the conformational and substituent dependences for α-, β- and γ-effects are similar to those for the 1-substituted butanes,[16] the primary interest will be on how these are affected by extending the chain to include the third dihedral angle. For all substituents and most values of φ_1 and φ_2, the calculated α-effects in Table 2 vary by less than 0.4 ppm with φ_3. However, for the sterically crowded *syn*-axial arrangements g^+g^- ($\varphi_1 = 60°$, $\varphi_2 = -60°$) and for tg^+ ($\varphi_1 = 180°$, $\varphi_2 = 60°$) orientations, the calculated $\Delta\delta_\alpha$ vary by as much as 6 and 2 ppm as φ_3 changes from g^+ to g^-, respectively. The calculated substituent dependences of α-effects are completely consistent with the experimental ones in Table 3 and follow the same trends (F > OH > CH_3 > CN) as the averaged ones in Table 1.

Since β-effects are relatively insensitive to φ_2,[16] it is not surprising to find only small variations with φ_3 in Table 2. The largest changes of *ca.* 0.8 ppm are also expected in the g^+g^- and tg^+ arrangements for φ_1 and φ_2. With one possible exception, the calculated trends in β-substituent effects in Table 3 follow the experimental ones in the order $CH_3 \geqslant$ OH > F > CN. The correspondence between the IGLO results and experimental data in Table 3 is poor for those examples having quaternary C1 carbons.

The IGLO γ-effects in Table 2 exhibit the smallest variations with φ_3, a possibly surprising result because of the sensitivity to both φ_1 and φ_2. The trends in the calculated and observed substituent γ-effects in Table 3 are somewhat conformation dependent. For tg^+c and

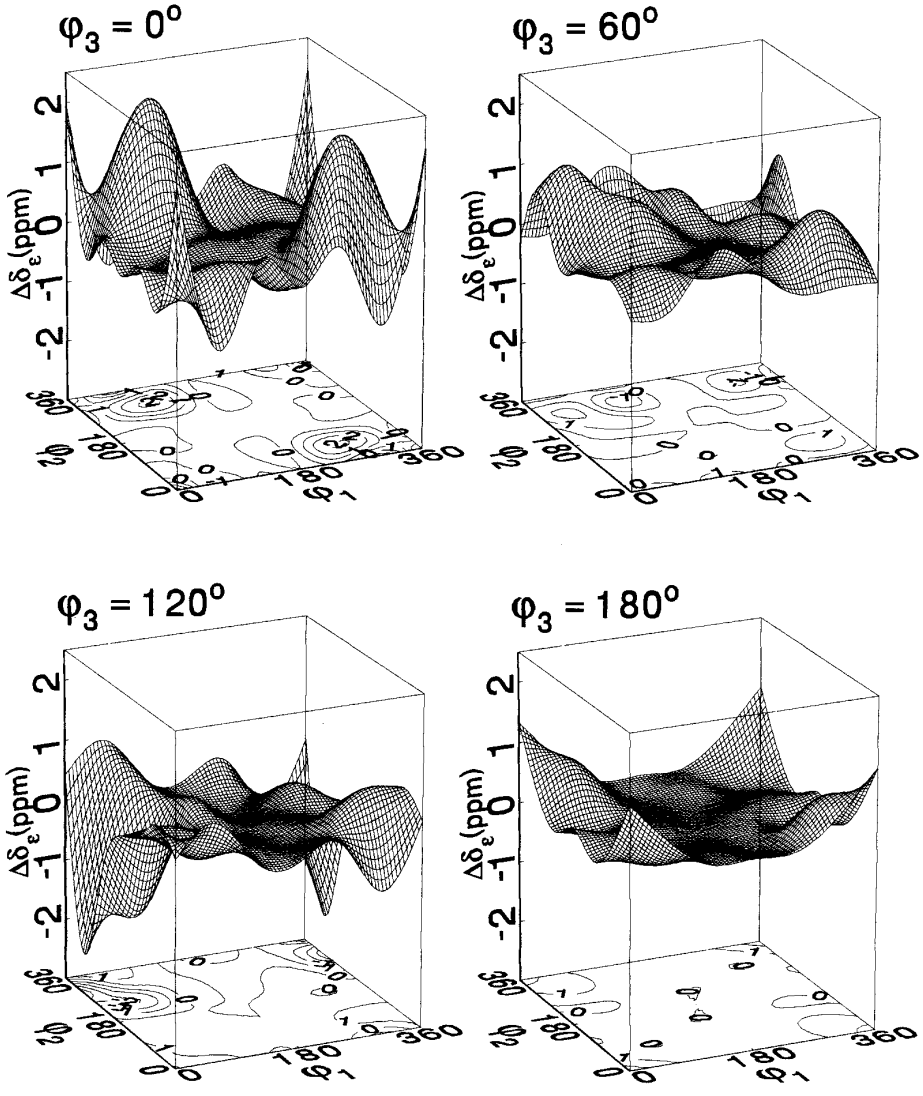

Figure 3. Calculated (IGLO/BS II′//HF/6–31G*) surface and contour plots of ε-effects $\Delta\delta_\varepsilon$ in ppm for the C6 carbon of *n*-hexane (**2**) plotted as a function of the dihedral angles φ_1 and φ_2 measured about the C2—C3 and C3—C4 bonds, respectively, for 0°, 60°, 120° and 180° values of φ_3 measured about the C4—C5 bond. The contour lines are separated by 0.5 ppm.

tg^+g^- conformations the order is $CH_3 > CN > OH > F$, whereas for $g^+g^+g^-$ (and possibly g^+g^+c) the CH_3 and CN order appears to be reversed ($CN > CH_3 > OH > F$).

δ-Effects

The IGLO results for $\Delta\delta_\delta$ of *n*-hexane are presented in Fig. 2 as a series of surface and contour plots *vs.* the dihedral angles φ_1 and φ_2 with φ_3 fixed at 0°, 60°, 120° and 180°. A spline algorithm was used to interpolate points at 10° intervals of φ_1 and φ_2.[29] The data for $\varphi_3 = 0°$ and 180° are symmetrical about a vertical plane passing through the diagonal $\varphi_1 = \varphi_2$. The surface and contour plots for $\varphi_3 = 300°$ and 240° are not reproduced here because they are related to those for 60° and 120°, respectively, by successive reflection in planes passing through $\varphi_1 = 180°$ and $\varphi_2 = 180°$. For example, in the $\varphi_3 = 60°$ plots the 3.0 ppm maximum which occurs for $\varphi_1 = 300°$ and $\varphi_2 = 60°$ (e.g. the $g^-g^+g^+$ conformation) would appear at $\varphi_1 = 60°$ and $\varphi_2 = 300°$ in plots for $\varphi_3 = 300°$ (e.g. the $g^+g^-g^-$ conformation depicted in Fig. 1). Other prominent features in Fig. 2 are the minima near -2 ppm in $g^+g^-g^+$ ($g^-g^+g^-$) conformations and the *ca.* -1 ppm minima predicted near $g^+g^+g^-$ conformations. Variations of the δ-effects with φ_3 in Table 2 are larger (*ca.* 5 ppm) for *n*-hexane than for the other three substituents.

The calculated δ-effects for the four substituents in Table 2 assume maximum values (3.0, 0.3, 2.6 and 2.2 ppm for $X = CH_3$, CN, OH, F, respectively) in $g^+g^-g^-$ arrangements. Minima (-1.9, -2.1, -0.8 and -1.4 ppm) occur for these substituents in $g^+g^-g^+$ conformations. In Table 3, it can be seen that the calculated IGLO δ-effects reproduce the trends in the experimental data for essentially all conformations. Again, the general trends follow those for the substituted pentanes ($CH_3 > OH > CN > F$) in Table 1.

The most pronounced conformational features in the IGLO δ-effects for substituted butanes were the *ca.* 2.5 ppm maxima for the *syn*-axial (g^+g^- and g^-g^+) arrangements of a δ-methyl. These were consistent with the experimental observations in substituted decalins.[16] However, the δ-methylene effects of all four 1-substituted pentanes are predicted to be strongly dependent on φ_3. The data in Table 3 comprise only nine sets of dihedral angles: g^+g^+c, $g^+g^+g^-$, g^+tg^+, g^+tt, g^+tg^-, tcg^+, tg^+c tg^+t and ttt. Six of these correspond to the 'standard' orientations in Fig. 1, but conspicuously missing are experimental data for any of the *syn*-axial arrangements $g^+g^-g^+$, g^+g^-t and $g^+g^-g^-$, as these should provide the extreme values for δ-effects. The predicted trends are qualitatively reproduced even though δ-effects are small. Possible exceptions are results for the 2-*exo*-substituted bicyclo[2.2.1]heptanes. The use of three dihedral angles in the substituted pentanes slightly improves the agreement between the calculated and experimental α- through γ-substituent effects in comparison with those for the substituted butanes.[17] The improvement is much greater for δ-effects because the δ-methylene carbons may be shielded or deshielded depending on φ_3. Consider, for example, δ-effects for the first 10 entries in Table 3. For the δ-methyl carbons of 1-substituted butanes only negative shifts (-0.5 to -0.7 ppm in Table 2) were predicted in g^+g^+ conformations. However, the δ-methylene carbons in the 1-substituted pentanes are found to be shielded or deshielded depending on the orientation of the terminal methyl. These results are in conformity with the experimental data in Table 3. Similarly, note the eight $\Delta\delta_\delta$ entries near conformations in which φ_1 and φ_2 are *trans* and *gauche*, respectively, in Table 2. The δ-methyl carbons in the butane series are all predicted to be deshielded (X = CN is exceptional) while all δ-methylene effects for the 1-substituted pentanes are predicted to be shielded, in conformity with all but one of the entries in Table 3.

ε-Effects

The conformational dependences of ε-substituent effects are of some interest because they seem not to have been examined previously. In Table 2 these vary with all three dihedral angles but cover the small range of *ca.* 1.5 to -1 ppm. Although the effects are small, they are not without interest and may be measurable for certain substituents and conformations.[30] The calculated IGLO ε-effects for the *n*-hexane/*n*-pentane model (as a representative example) are presented in Fig. 3. The dependence of $\Delta\delta_\varepsilon$ on the dihedral angles φ_1 and φ_2 is depicted by surface and contour plots for φ_3 having the values 0°, 60°, 120° and 180°. Prominent features of these plots are the *ca.* 2 and 1 ppm maxima and -1 and -2.3 ppm minima for g^+g^-c, cg^+s^-, $g^+g^+g^-$ and cg^-s^+ conformations, respectively. Several values of ε-effects for methylene carbons are given in Table 3 for substituted *trans*-decalins. Because the effects are small in these conformations and the calculations apply to an ε-methyl carbon, the correlation is not good. Furthermore, the ε-effects of methylenes probably depend on a fourth dihedral angle.

A better comparison might be provided by those cases in which the ε-carbon is a methyl group. Table 4 gives the calculated and experimental α-through ε-substituent effects for a series of dimethyl-*trans*-decalins (DMTD) having ε-methyl carbons. Also included are entries for two *trans*-decalins (TD) with hydroxyl substituents at the C3 position. In all but two of the examples in Table 4, the magnitudes of ε-effect are less than 0.2 ppm, which are probably too small for meaningful comparisons. Of the various conformations which are

Table 4. Comparison of calculated α- through ε-effects (IGLO/BS II′//HF/6–31G*) for substituted pentanes with experimental data for several disubstituted *trans*-decalins having ε-methyl carbons[a]

	Dihedral angles[c]			$\Delta\delta_\alpha$		$\Delta\delta_\beta$		$\Delta\delta_\gamma$		$\Delta\delta_\delta$		$\Delta\delta_\varepsilon$	
Compound[b]	φ_1	φ_2	φ_3	Calc.	Expt.	Calc.	Expt.	Calc.	Expt.	Calc.	Expt.	Calc.	Expt.
2ax, 5eq-DMTD	73	57	180	6.0	−1.3	6.6	7.4	−4.1	−6.3	−0.5	0.9	0.0	0.1
2ax, 9eq-DMTD	55	176	179	6.4	6.1	5.8	8.8	−4.8	−0.7	0.2	−0.1	0.2	−0.1
2eq, 9eq-DMTD	58	179	180	6.4	3.3	5.9	6.0	−4.7	−3.9	0.2	0.0	0.1	0.1
2ax, 7eq-DMTD	71	178	176	7.0	−1.3	6.7	2.7	−3.8	−7.7	0.2	0.9	0.1	0.1
2ax, 5eq-DMTD	179	57	72	8.0	4.0	8.3	3.7	−0.7	−0.6	0.5	0.3	0.0	0.0
2eq, 5eq-DMTD	178	58	178	8.0	3.0	8.4	9.4	−0.7	−0.6	0.5	−0.1	0.1	0.2
2ax, 9eq-DMTD	179	176	55	8.7	0.5	8.3	2.7	−1.2	−2.7	0.0	−0.5	0.0	0.1
2ax, 7eq-DMTD	176	178	71	8.6	3.6	8.3	6.2	−1.2	−0.8	0.0	0.2	0.0	−0.1
2eq, 9eq-DMTD	180	179	58	8.6	5.9	8.2	8.6	−1.2	−0.6	0.0	−0.3	0.0	0.0
2eq, 7eq-DMTD	179	180	181	8.6	3.2	8.3	6.2	−1.2	−0.5	0.0	0.0	0.0	0.5
3ax-OH-6-ME-TD	70	54	69	42.9	39.4	7.6	6.7	−5.2	−6.5	−0.4	−0.2	0.4	−1.0
3eq-OH-6-ME-TD	183	55	68	45.1	43.8	7.6	9.1	−3.6	−2.7	1.0	−0.9	0.1	0.0

[a] Angles are in degrees and substituent effects in ppm.
[b] All data taken from Whitesell and Minton (footnote b of Table 3).
[c] See footnote c of Table 3.

represented by the data in Table 4, none correspond to situations in which ε-effects are larger than 0.4 ppm. For the latter case, the experimentally inferred $\Delta\delta_\varepsilon$ is of opposite sign. In contrast to the computed δ-effects in Table 3, those in Table 4 are poor as all δ-carbons are either tertiary or quaternary.

LOCAL BOND CONTRIBUTIONS IN STERICALLY CROWDED ARRANGEMENTS OF *N*-HEXANE

There has been much interest in the role of steric crowding on ^{13}C NMR substituent effects.[2–4,9–12] It will be useful to examine the IGLO local bond contributions (LBC) associated with δ- and ε-effects. Since the less sterically crowded conformations have smaller magnitudes for δ- and ε-effects, it is more difficult to sort out the significance of the various local bond contributions. In the IGLO method, chemical shielding at a particular carbon is the sum of contributions from inner shells, localized bonds and lone-pairs.[22,23] The LBCs include both diamagnetic and paramagnetic contributions but are dominated by the latter. The substituent and conformational changes in the ^{13}C chemical shifts of substituted hydrocarbons are primarily reflected in the LBCs of the four bonds on carbon. Of interest here are the changes in the local bond contributions for δ- and ε-effects in the sterically crowded *syn*-axial arrangements, e.g., $\varphi_1 = 60°$ and $\varphi_2 = 300°$ ($g^+g^-g^+$, g^+g^-t and $g^+g^-g^-$ conformations). For these conformations of *n*-hexane the HF/6–31G* geometries are depicted in Fig. 4. Clearly, the first of these has the greatest steric crowding leading to an expansion of the C2—C3—C4 bond angle to 126° and compression of the C5—H9 bond to 1.079 Å. The latter is almost 0.01 Å smaller than the other C—H bonds in the molecule.

Table 5 gives the changes $\Delta\delta_\delta^{LBC}$ in each of the four IGLO local bond contributions at the C5 carbon of *n*-hexane. These were obtained for the ($g^+g^-g^+$, g^+g^-t and $g^+g^-g^-$) conformations of *n*-pentane on replacement of a hydrogen (on C2) by a *gauche*-methyl. The totals for each of the four bonds are given at the bottom of the table. For the $g^+g^-g^+$ conformation of *n*-hexane, the changes $\Delta\delta_\delta^{LBC}$ of the four bonds on C5 add up to −1.3 ppm. This compares with a total predicted δ-effect of −1.9 ppm in Table 2. For this conformation in Fig. 4

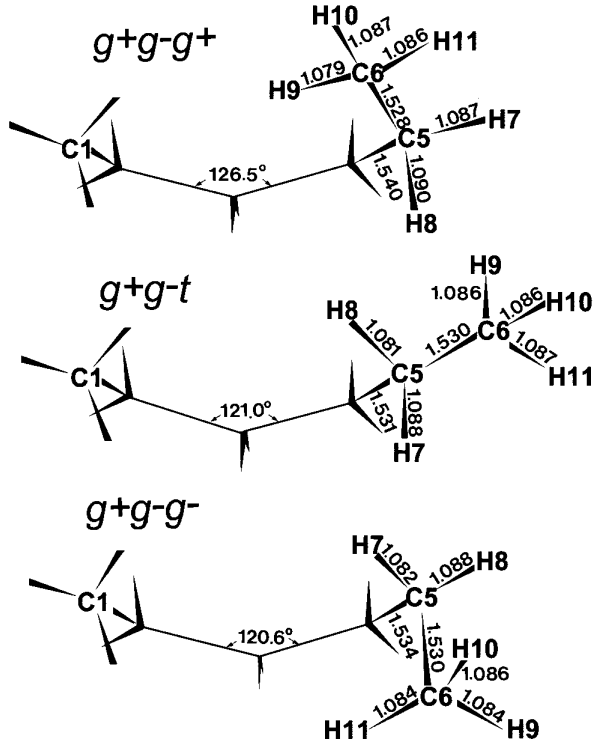

Figure 4. Bond orientations and representative internuclear separations (obtained at the HF/6–31G* level) for sterically crowded (a) $g^+g^-g^+$, (b) g^+g^-t and (c) $g^+g^-g^-$ conformations of *n*-hexane.

the C5—H7 and C5—H8 bonds point way from the C1 methyl group. The changes in the LBCs are shielding for both C—H bonds contributing a total of −0.7 ppm to the total $\Delta\delta_\delta$ at C5. The C4—C5 bond provides an equal amount. Rotation of the C6 methyl group by 120° about the C4—C5 bond produces the g^+g^-t conformation in Fig. 4. The C5—H8 bond (which points toward the C1 methyl) is shortened and $\Delta\delta_\delta^{LBC}$ is positive (+0.8 ppm, about half of the deshielding predicted for C5 in this conformation). The contribution from C5–H7 corresponds to a small shielding contribution. Another 120° rotation about the C4—C5 bond leads to the $g^+g^-g^-$ conformation depicted in Fig. 4. In this conformation the C5—H7 bond points toward the substituent and C5—H8 points away. The $\Delta\delta_\delta^{LBC}$ for the first of these in Table 5 again corresponds to deshielding by 1.6 ppm, a substantial contribution to the total in Table 2. In this case the C5—H8 bond pointing away from the C1 methyl provides a small positive contribution.

Table 5. Changes in the IGLO local bond contributions $\Delta\delta^{LBC}$ for each of the four bonds at the C5 and C6 carbon atoms in *syn*-axial arrangements of *n*-hexane

δ-Effects, $\Delta\delta_\delta^{LBC}$ (ppm)				ε-Effects, $\Delta\delta_\varepsilon^{LBC}$ (ppm)			
Bond	$g^+g^-g^+$	g^+g^-t	$g^+g^-g^-$	Bond	$g^+g^-g^+$	g^+g^-t	$g^+g^-g^-$
C5—H6	0.1	0.5	−0.1	C5—C6	−0.2	0.3	0.2
C5—H7	−0.6	−0.2	1.6	C6—H9	0.7	0.0	−0.1
C5—H8	−0.1	0.8	0.2	C6—H10	0.3	0.2	0.1
C4—C5	−0.7	0.1	0.7	C6—H11	−0.2	0.2	0.3
Total	−1.3	1.2	2.4	Total	0.6	0.7	0.5

Also included in Table 5 are the $\Delta\delta_{\varepsilon}^{LBC}$ associated with the four bonds on the C6 carbon of *n*-hexane. The closest approach between the C1 and C6 methyl groups occurs for the $g^+g^-g^+$ conformation and involves the C6—H9 bond, which is compressed to 1.079 Å. From the data in Table 5 it can be seen that this bond contributes 0.7 ppm to the deshielding of the C6 carbon in this arrangement and it is two to three times larger in magnitude than the other changes in the local bond contributions.

CONCLUSION

Ab initio MO calculations performed here at the HF/6–31G* and IGLO Basis Set II′ level provide a satisfactory description of ^{13}C chemical shifts and α-, β-, γ- and δ-effects for 1-substituted pentanes with CH_3, CN, OH and F substituents at the C1 positions. The isotropic ^{13}C chemical shifts for the substituted pentanes were examined as functions of the dihedral angles φ_1, φ_2 and φ_3 about the C1—C2, C2—C3 and C3—C4 bonds, respectively. Of particular interest are the computed δ- and ε-effects. Even though δ-methylene effects cover a small range except for the unusual cases of *syn*-axial arrangements, the recognition of their dependence on three dihedral angles offers additional potential for their use in conformational analyses, especially when used in combination with other data. This is probably the first investigation of the substituent and conformational dependences of ε-effects. These depend on at least three dihedral angles, but this complexity combined with small magnitudes probably precludes any application in stereochemical applications. An analysis of the IGLO local bond contributions to δ- and ε-effects in sterically crowded *syn*-axial arrangements ($\varphi_1 = 60°$, $\varphi_2 = 300°$) suggests that the compressed C—H bonds pointing toward the substituent provide deshielding contributions whereas those pointing away are often shielding.

Acknowledgements

Appreciation is extended to Professor W. Kutzelnigg and Dr M. Schindler for permission to use the IGLO program. The National Science Foundation is acknowledged for grants to assist in the purchase of the computers used in this study.

REFERENCES

1. D. M. Grant and E. G. Paul, *J. Am. Chem. Soc.* **86**, 2984 (1964); E. G. Paul and D. M. Grant, *J. Am. Chem. Soc.* **85**, 1701 (1963).
2. D. M. Grant and B. V. Cheney, *J. Am. Chem. Soc.* **89**, 5315 (1967).
3. R. Hagan and J. D. Roberts, *J. Am. Chem. Soc.* **91**, 4504 (1969); J. I. Kroschwitz, M. Winokur, H. J. Reich and J. D. Roberts, *J. Am. Chem. Soc.* **91**, 5927 (1969); J. D. Roberts, F. J. Weigert, J. I. Kroschwitz and H. J. Reich, *J. Am. Chem. Soc.* **92**, 1338 (1970); J. B. Grutzner, M. Jautelat, J. B. Dence, R. A. Smith and J. R. Roberts, *J. Am. Chem. Soc.* **92**, 7107 (1970).
4. J. B. Stothers, *Carbon-13 NMR Spectroscopy*. Academic Press, New York (1972).
5. L. P. Lindeman and J. Q. Adams, *Anal. Chem.* **43**, 1245 (1971).
6. J. T. Clerc, E. Pretsch and S. Sternhell, *^{13}C Kernrezonanzspektroskopie*. Akademische Verlagsgesellschaft, Franffurt am Main (1973).
7. H. N. Cheng and S. J. Ellingsen, *J. Chem. Inf. Comput. Sci.* **23**, 197 (1983).
8. F. Imashiro, Y. Masuda, M. Honda and S. Obara, *J. Chem. Soc., Perkin Trans. 2* 1535 (1993).
9. E. Eliel and K. M. Petrusiewicz, in Topics in Carbon-13 NMR Spectroscopy, edited by G. C. Levy, Vol. 3, p. 172. Wiley–Interscience, New York (1979).
10. For reviews of the stereochemistry of α-, β-, γ- and δ-effects, see H. Duddeck, *Top. Stereochem.* **16**, 219 (1986) and A. P. Marchand, *Stereochemical Applications of NMR Studies in Rigid Bicyclic Systems*. Verlag Chemie, Deerfield Beach, FL (1982).
11. K. Pihlaja and E. Kleinpeter, *Carbon-13 NMR Chemical Shifts in Structural and Stereochemical Analysis*. VCH, New York (1994).
12. M. Barfield and S. Yamamura, *J. Am. Chem. Soc.* **112**, 4747 (1990).
13. M. Barfield, in *Nuclear Magnetic Shieldings and Molecular Structure*, edited by J. A. Tossell, p. 523. Kluwer, Boston (1993).
14. M. Barfield, *J. Am. Chem. Soc.* **115**, 6916 (1993).
15. D. Jiao, M. Barfield, J. E. Combariza and V. J. Hruby, *J. Am. Chem. Soc.* **114**, 3639 (1992); D. Jiao, M. Barfield and V. J. Hruby, *Magn. Reson. Chem.* **31**, 75 (1993); D. Jiao, M. Barfield and V. J. Hruby, *J. Am. Chem. Soc.* **115**, 10883 (1993).
16. M. Barfield, *J. Am. Chem. Soc.* **117**, 2862 (1995).
17. M. Barfield and P. Fagerness, *J. Am. Chem. Soc.* **119**, 8699 (1997).
18. H. Kurosu, I. Ando and G. A. Webb, *Magn. Reson. Chem.* **31**, 399 (1993); R. Born, H. W. Spiess, W. Kutzelnigg, U. Fleischer and M. Schindler, *Macromolecules* **27**, 1500 (1994); R. Born and H. W. Spiess, *Macromolecules* **28**, 7785 (1995); M. Wada, M. Sakurai and Y. Watanabe, *Magn. Reson. Chem.* **33**, 453 (1995); A. C. de Dios and E. Oldfield, *J. Am. Chem. Soc.* **116**, 5307 (1994); A. C. de Dios and C. J. Jameson, *Annu. Rep. NMR Spectrosc.* **29**, 1 (1994).
19. M. J. Frisch, G. W. Trucks, H. B. Schlegel, P. M. W. Gill, B. G. Johnson, M. W. Wong, J. B. Foresman, M. A. Robb, M. Head-Gordon, E. S. Replogle, R. Gomperts, J. L. Andres, K. Raghavachari, J. S. Binkley, C. Gonzalez, R. L. Martin, D. J. Fox, D. J. Defrees, J. Baker, J. J. P. Stewart and J. A. Pople, *Gaussian 92*/DFT, *Revision G.3*. Gaussian, Pittsburgh, PA (1993).
20. M. J. Frisch, G. W. Trucks, H. B. Schlegel, P. M. W. Gill, B. G. Johnson, M. A. Robb, J. R. Cheeseman, T. Keith, G. A. Petersson, J. A. Montgomery, K. Raghavachari, M. A. Al-Laham, V. G. Zakrzewski, J. V. Ortiz, J. B. Foresman, C. Y. Peng, P. Y. Ayala, W. Chen, M. W. Wong, J. L. Andres, E. S. Replogle, R. Gomperts, R. L. Martin, D. J. Fox, J. S. Binkley, D. J. Defrees, J. Baker, J. P. Stewart, M. Head-Gordon, C. Gonzalez and J. A. Pople, *Gaussian 94, Revision B.3*. Gaussian, Pittsburgh, PA (1995).
21. W. J. Hehre, R. Ditchfield and J. A. Pople, *J. Chem. Phys.* **56**, 2257 (1972); P. C. Hariharan and J. A. Pople, *Theor. Chim. Acta* **28**, 213 (1973).
22. W. Kutzelnigg, *Isr. J. Chem.* **19**, 192 (1980); M. Schindler and W. Kutzelnigg, *J. Chem. Phys.* **76**, 1919 (1982); M. Schindler and W. Kutzelnigg, *Mol. Phys.* **48**, 781 (1983); M. Schindler and W. Kutzelnigg, *J. Am. Chem. Soc.* **105**, 1360 (1983).
23. For reviews of IGLO, see W. Kutzelnigg, U. Fleischer and M. Schindler, in *NMR Basic Principles and Progress*, edited by P. Diehl, E. Fluck and R. Kosfeld, Vol. 23, p. 165. Springer, Berlin (1990); W. Kutzelnigg, Ch. van Wüllen, U. Fleischer, R. Franke and T. v. Mourik, in *NMR Shieldings and Molecular Structure*, edited by J. A. Tossell, p. 141. Kluwer, Norwell, MA (1993); W. Kutzelnigg, U. Fleischer and Ch. van Wüllen, *Encycl. Magn. Reson.* **7**, 4284 (1996).
24. Aa. E. Hansen and M. Bilde, *Encycl. Magn. Reson.* **7**, 4292 (1996).
25. P. Pulay and J. F. Hinton, *Encycl. Magn. Reson.* **7**, 4334 (1996).
26. For reviews of the theory of shielding, see, for example, C. J. Jameson, *Nuclear Magnetic Resonance*, Specialist Periodical Reports, No. 26. Chemical Society, London (1997), and previous chapters in this series; G. A. Webb, *Encycl. Magn. Reson.* **7**, 4307 (1996); D. B. Chesnut, *Annu. Rep. NMR Spectrosc.* **29**, 71 (1994).
27. S. Huzinaga, *Gaussian Basis Sets for Molecular Calculations*. Elsevier, New York (1984).
28. A. K. Jameson and C. J. Jameson, *Chem. Phys. Lett.* **134**, 461 (1987).
29. *Axum: Technical Graphics and Data Analysis*, 2nd ed. TriMatrix, Seattle, WA (1992).
30. P. R. Seidl, K. Z. Leal, V. E. U. Costa and M. E. S. Möllmann, *Magn. Reson. Chem.* **31**, 241 (1993); P. R. Seidl, K. Z. Leal, V. E. U. Costa and M. E. S. Möllmann, *Magn. Reson. Chem.* **36**, 261 (1998).

